Effects of optimal control over thermoconvective patterns

M. C. Navarro and H. Herrero
Departamento de Matemáticas, Facultad de Ciencias Químicas, Universidad de Castilla-La Mancha, 13071 Ciudad Real, Spain
(Received 23 January 2007; revised manuscript received 17 April 2007; published 22 June 2007)

This paper shows that optimal control techniques can be used to avoid some pattern formation in a Rayleigh-Bénard problem with horizontal temperature gradient. Appropriate thermal boundary conditions determined by these techniques lead to new strong controlled basic states with reduced pattern and for which the thermoconvective instability is avoided.

DOI: 10.1103/PhysRevE.75.067203 PACS number(s): 05.45.Gg, 47.85.L−, 02.70.Jn, 44.25.+f

Thermoconvective flows occur frequently in nature, in industrial applications or in daily life. For instance, thermoconvective instabilities are responsible for undesirable convective states in some industrial processes such as crystal growth, laser welding or alloy manufacturing. In those processes it is important to avoid convective patterns in order to achieve homogeneous and resistant materials [1–4]. Optimal control techniques can be useful for this. Classically, the problem is stated as a fluid layer heated uniformly from below [5–7]. A conductive state becomes unstable when temperature gradients go beyond a certain threshold. The onset of motion is caused by two different effects: gravity and capillary forces. A more general approach considers thermoconvective instabilities where a basic dynamic flow is imposed through nonzero horizontal temperature gradients [8–10]. In this last problem the appearance of patterns is accompanied by an increase of the enstrophy in the flow. We look for the boundary conditions that minimize the enstrophy of the flow by solving numerically the optimality conditions found in Ref. [11]. We have proven that basic state patterns disappear and some of the controlled states obtained are highly stable in situations where enstrophy reduction is efficient.

The physical setup considered consists of a horizontal fluid layer in a rectangular container of width l (x coordinate) and depth d (z coordinate), $\Omega' = [0,l] \times [0,d]$. The top boundary is open to the atmosphere; at the bottom the profile is linear, with a temperature $T_{\max}$ in the left lateral wall while the right lateral wall is at $T_{\min}$ and the environment at T_0. We define $\triangle T = T_{\max} - T_0$ and $\triangle T_h = T_{\max} - T_{\min}$.

The system evolves according to the momentum and mass balance equations and to the energy conservation principle. In the equations governing the system u_x and u_z are the components of the velocity field $\mathbf{u}$ of the fluid, T is the temperature, p is the pressure, $\mathbf{x} = (x,z)$ are the spatial coordinates and t is the time. Magnitudes are expressed in dimensionless form after rescaling in the following way: $\mathbf{x}' = \mathbf{x}/d$, $t' = \kappa t/d^2$, $\mathbf{u}' = d\mathbf{u}/\kappa$, $p' = d^2 p/(\rho_0 \kappa \nu)$, $\Theta = (T - T_0)/\triangle T$. Here κ is the thermal diffusivity, ν is the kinematic viscosity of the liquid, and ρ_0 is the mean density at ambient temperature T_0.

The governing dimensionless steady state equations (the primes in the corresponding fields have been dropped) are

$$\nabla \cdot \mathbf{u} = 0, \quad \mathbf{u} \cdot \nabla \Theta = \nabla^2 \Theta, \tag{1}$$

$$(\mathbf{u} \cdot \nabla)\mathbf{u} = \mathrm{Pr}(-\nabla p + \nabla^2 \mathbf{u} + \mathrm{Ra}\Theta \mathbf{e}_z). \tag{2}$$

Here the Oberbeck-Bousinesq approximation has been used. This consists in considering the following density dependence on temperature $\rho = \rho_0[1 - \alpha(\Theta - T_0)]$, where α is the thermal expansion coefficient, only in the buoyant term. The following dimensionless numbers have been introduced:

$$\mathrm{Pr} = \frac{\nu}{\kappa}, \quad \mathrm{Ra} = \frac{g\alpha \Delta T d^3}{\kappa \nu},$$

where g is the gravity constant, Pr is the Prandtl number, and Ra the Rayleigh number representative of the buoyancy effect (the bifurcation parameter in the stability analysis).

Moving on to the boundary conditions (bc), the top boundary is flat and open to the atmosphere, which implies the following conditions on velocity:

$$u_z = 0, \quad \partial_n u_x = 0 \text{ on } z = 1. \tag{3}$$

The remaining boundary conditions correspond to rigid walls and are expressed as follows:

$$u_x = u_z = 0 \text{ on } z = 0, \quad x = 0, \quad \text{and } x = \gamma, \tag{4}$$

where $\gamma = l/d$ is the aspect ratio. For temperature we take the dimensionless form of Newton's law for heat exchange at the surface with a heat flux h

$$\partial_n \Theta = -\mathrm{Bi}\Theta + \mathrm{Bi}h, \quad \text{on } z = 1, \tag{5}$$

where Bi is the Biot number and h is the heat flux that serves as the control function. In our notation $h = 0$ for the uncontrolled states and $h \neq 0$ is the function resulting from the optimal control procedure in the controlled states. At the bottom the following Dirichlet condition is imposed,

$$\Theta = \Theta^1(x), \quad \text{on } z = 0, \tag{6}$$

where $\Theta^1(x)$ is a quasilinear function, i.e., it is a linear profile $\Theta^1(x) = 1 - x\Delta T_h/(\Delta T \gamma)$ for $0.05\gamma \leqslant x \leqslant 0.95\gamma$ and a second order polynomial that matches the linear profile with the boundaries satisfying $\partial_n \Theta^1|_{x=0,\gamma} = 0$. In the lateral walls, insulating boundary conditions are considered,

$$\partial_n \Theta = 0 \text{ on } x = 0 \text{ and } x = \gamma. \tag{7}$$

This system has been solved numerically by a Chebyshev collocation method explained in Refs. [9,12,13]. This approximation is given by four fields $u_x(x,z)$, $u_z(x,z)$, $p(x,z)$, and $\Theta(x,z)$ which are expanded in a truncated series of orthonormal Chebyshev polynomials. The numerical solutions of this system [Eqs. (1) and (2) and boundary conditions (3)–(7)] are the basic states that we name $\mathbf{u}^b(x,z) = [u_x^b(x,z), u_z^b(x,z)]$, $\Theta^b(x,z)$, and $p^b(x,z)$. As in Refs. [8–10], we have found two types of solutions (basic states) depending on the parameters: corotating rolls (linear flow), which

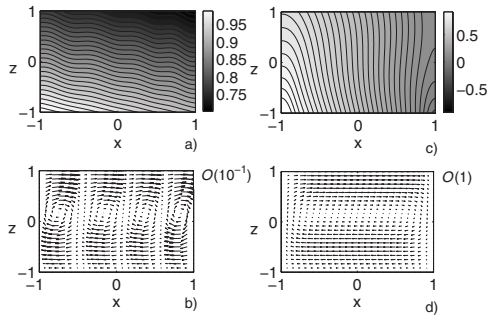

FIG. 1. (a) Isotherms for a linear flow basic state. The parameters are Bi=0.3, γ=11.76, Ra=3200, and $\Delta T_h/\Delta T$=0.08; (b) velocity field of the same basic state corresponding to corotating rolls; (c) isotherms for a return flow basic state. The parameters are Bi=0.3, γ=6, Ra=1125, and $\Delta T_h/\Delta T$=1; (d) velocity field of the same basic state corresponding to a single roll.

can be seen in Figs. 1(a) (isotherms) and 1(b) (velocity field), or a single roll (return flow) which can be seen in Figs. 1(c) (isotherms) and 1(d) (velocity field). We have used the terminology "linear" and "return flow" introduced in Ref. [8]. We have a return flow when along the vertical axis there are changes in the sign of the temperature gradient. When the basic state does not present this feature we say that it is a linear flow.

We have studied the linear stability of these basic states by perturbating them with a vector field

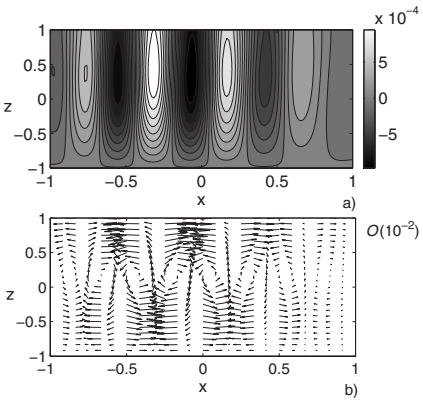

FIG. 2. (a) Isotherms for the growing perturbation after the bifurcation. The parameters are Bi=0.3, γ=11.76, Ra=3245, and $\Delta T_h/\Delta T$=0.08; (b) velocity field of the same growing perturbation.

$$u_x(x,z) = u_x^b(x,z) + \bar{u}_x(x,z)e^{\sigma t}, \tag{8}$$

and similarly for u_z, Θ, and p. Expression (8) and similar expressions for the rest of the fields are substituted in the basic equations (1) and (2) and boundary conditions. The resulting system is linearized and an eigenvalue problem in σ is obtained:

$$\nabla \cdot \bar{\mathbf{u}} = 0, \quad \mathbf{u}^b \cdot \nabla\bar{\Theta} + \bar{\mathbf{u}} \cdot \nabla\Theta^b - \nabla^2\bar{\Theta} = -\sigma\bar{\Theta}, \tag{9}$$

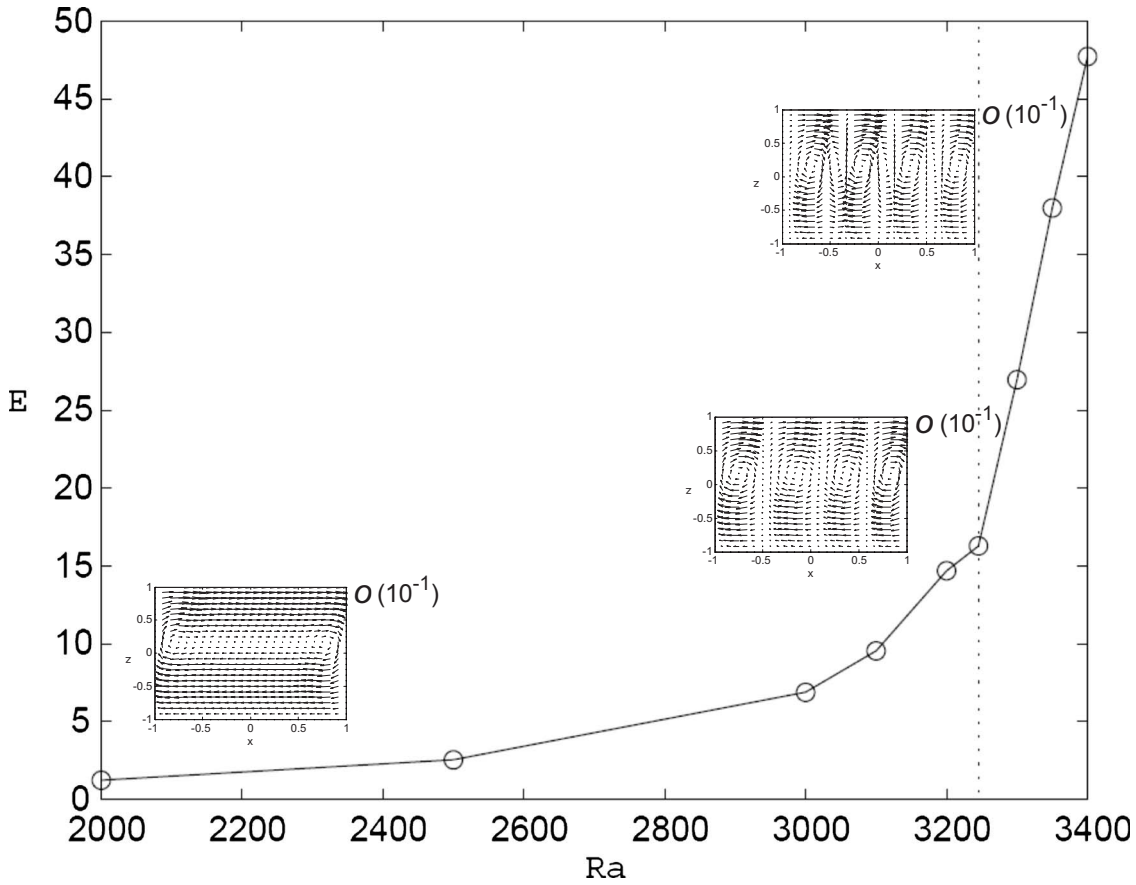

FIG. 3. Enstrophy (E) as a function of the Rayleigh number Ra in the linear flow case. Dashed vertical line: critical Rayleigh number. The parameters are Bi=0.3, γ=11.76, and $\Delta T_h/\Delta T$=0.08. Velocity fields plots for Ra=2000, 3200, and 3300 are included.

TABLE I. Critical Rayleigh number for the controlled solutions at Bi=0.3, γ=11.76, and $\Delta T_h/\Delta T$=0.08 at δ=0.001 for different order expansions in N and M.

	$M=13$	$M=15$	$M=17$	$M=19$	$M=21$
$N=25$	2938.78	2934.78	2932.09	2930.19	2928.92
$N=27$	2958.32	2959.00	2959.49	2959.78	2959.98
$N=33$	2960.17	2960.46	2960.76	2960.95	2961.15
$N=37$	2956.26	2953.33	2951.48	2950.2	2949.37
$N=39$	2959.05	2953.33	2956.75	2956.26	2955.87
$N=41$	2955.37	2954.93	2954.68	2954.56	2954.40

$$(\mathbf{u}^b\cdot\nabla)\bar{\mathbf{u}}+(\bar{\mathbf{u}}\cdot\nabla)\mathbf{u}^b-\mathrm{Pr}(-\nabla\bar{p}+\nabla^2\bar{\mathbf{u}}+\mathrm{Ra}\bar{\Theta}\mathbf{e}_z)=-\sigma\bar{\mathbf{u}}, \tag{10}$$

with the corresponding boundary conditions.

The system is solved with the same Chebyshev-collocation method as the one used to obtain the basic states [9,13]. In the case of the corotating rolls, the bifurcations are stationary and the critical Rayleigh number for Bi=0.3, γ =11.76 and $\triangle T_h/\triangle T$=0.08, for instance, is Ra_c=3245. The growing perturbation after the bifurcation can be seen in Fig. 2. The new structure of the flow will be a linear combination of the basic state and the growing perturbation. The return flow state is stable for any value of Ra, i.e., there is no bifurcation. Another main point, apart from reducing patterns, is to study the effect of control over the instability. So we will concentrate on the corotating rolls case hereafter.

Optimal control problem. If we consider the measure of vorticity ($\omega=\nabla\times\mathbf{u}$), $E(\mathbf{u})=\int_\Omega|\nabla\times\mathbf{u}|^2d\Omega$ which is called enstrophy, we observe in a plot of enstrophy depending on the Rayleigh number (Fig. 3) that the appearance of patterns is accompanied by an increase of the enstrophy in the flow. This suggests that by reducing the enstrophy we could obtain states for which patterns will also be reduced. For this reason we look for the control function h on the top boundary which minimizes the enstrophy of the flow. We state the optimal control problem as in Ref. [11].

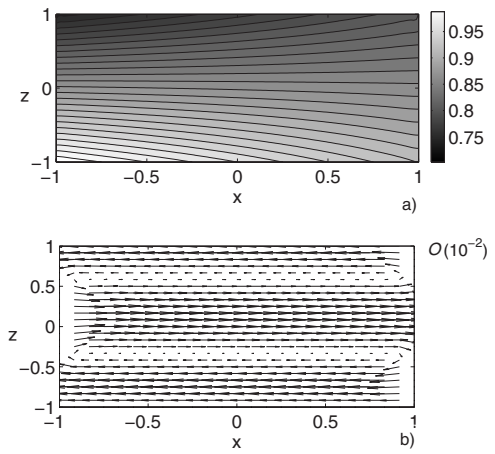

FIG. 4. (a) Isotherms in the controlled linear flow case for $\delta=5\times10^{-4}$; (b) velocity field in the same case. The parameters are Bi=0.3, γ=11.76, Ra=3200, and $\Delta T_h/\Delta T$=0.08.

Minimize $J(\mathbf{u},\Theta,h)=\frac{1}{2}\int_\Omega|\nabla\times\mathbf{u}|^2d\Omega+\frac{\delta}{2}\int_0^\gamma h^2dx$, subject to the state

$$\nabla\cdot\mathbf{u}=0,\quad \mathbf{u}\cdot\nabla\Theta-\nabla^2\Theta=0, \tag{11}$$

$$(\mathbf{u}\cdot\nabla)\mathbf{u}+\mathrm{Pr}(\nabla p-\nabla^2\mathbf{u}-\mathrm{Ra}\Theta\mathbf{e}_z)=0, \tag{12}$$

with boundary conditions as follows:

$$u_x=u_z=0,\quad \partial_n\Theta=0 \text{ on } x=0 \text{ and } x=\gamma, \tag{13}$$

$$u_x=u_z=0,\quad \Theta-\Theta_1=0 \text{ on } z=0, \tag{14}$$

$$u_z=0,\quad \partial_n u_x=0,\quad \partial_n\Theta+\mathrm{Bi}\Theta-\mathrm{Bi}h=0 \text{ on } z=1, \tag{15}$$

where h is a temperature control using radiational heating or cooling. In the cost functional J, the term $E(\mathbf{u})=\int_\Omega|\nabla\times\mathbf{u}|^2d\Omega$ is the enstrophy previously introduced, the term $\int_0^\gamma h^2dx$ is the measure of the magnitude of the control and the penalizing parameter δ adjusts the size of the terms in the cost.

Reference [11] proves the existence of solutions for the optimal control problem and provides the optimality conditions. These conditions include the above equations and boundary conditions together with the new equations and boundary conditions for the control $h(x)$ and the auxiliary fields $\xi(x,z)=[\xi_x(x,z),\xi_z(x,z)]$, $\pi(x,z)$ and $\lambda(x,z)$:

$$\nabla\cdot\xi=0,\quad -\mathbf{u}\cdot\nabla\lambda=\nabla^2\lambda+\mathrm{Pr}\,\mathrm{Ra}\xi\mathbf{e}_z, \tag{16}$$

$$-(\mathbf{u}\cdot\nabla)\xi+(\nabla\mathbf{u})^t\xi=\mathrm{Pr}(-\nabla\pi+\nabla^2\xi)-\lambda\nabla\Theta-[\nabla\mathbf{x}(\nabla\mathbf{x}\mathbf{u})], \tag{17}$$

$$\xi_x=\xi_z=0,\quad \partial_n\lambda=0 \text{ on } x=0 \text{ and } x=\gamma, \tag{18}$$

$$\xi_x=\xi_z=0,\quad \lambda=0 \text{ on } z=0, \tag{19}$$

$$\xi_z=0,\quad \partial_n\xi_x=0,\quad \partial_n\lambda=-\mathrm{Bi}\lambda,\quad \mathrm{Bi}\lambda-\delta h=0 \text{ on } z=1. \tag{20}$$

This optimality system has been solved numerically by a Chebyshev collocation method [9,12,13]. The approximation is given by nine fields u_x, u_z, p, Θ, ξ_x, ξ_z, π, λ, and h, which are expanded in a truncated series of orthonormal Chebyshev polynomials. The convergence of the numerical method is tested by comparing the differences in the value of the critical Rayleigh number for different orders of expansions in

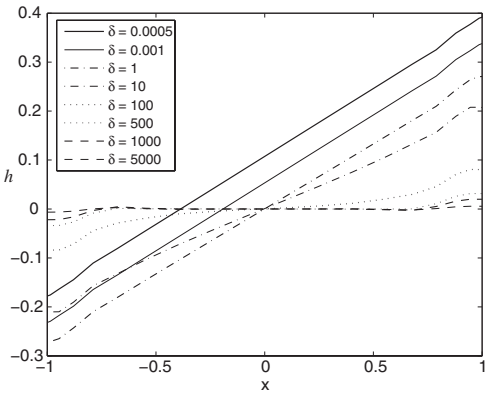

FIG. 5. Control function h in the case Bi=0.3, γ=11.76, Ra =3200, $\Delta T_h/\Delta T$=0.08 for different values of δ.

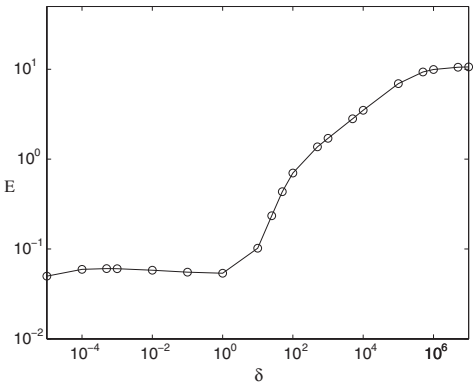

FIG. 6. Enstrophy (E) as a function of the penalizing parameter δ. The parameters are Bi=0.3, γ=11.76, Ra=3200, and $\Delta T_h/\Delta T$ =0.08.

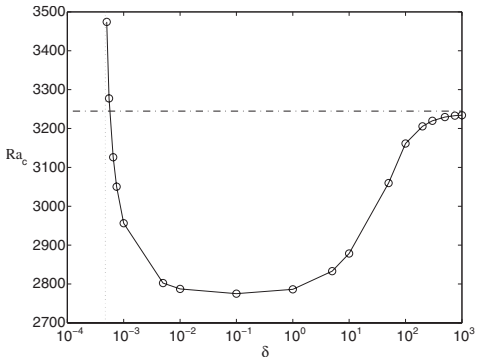

FIG. 7. Solid line: critical Rayleigh number for the controlled states for different values of the penalizing parameter δ. Dashed horizontal line: critical Rayleigh number for the uncontrolled state. Dotted vertical line: asymptotic value of δ limit of bifurcation zone. The values of the parameters are Bi=0.3, γ=11.76, and $\Delta T_h/\Delta T$ =0.08.

Chebyshev polynomials. These values are shown in Table I for several consecutive expansions, varying the number of polynomials taken in the x (N) and z (M) coordinates. Convergence is attained, with a relative degree of precision, for Ra_c in the region of 10^{-4}. We can see that if M is increased there will be no significant difference between successive expansions. Convergence is satisfactory from N=37 and M =13, and these are the orders used in the numerical computations throughout the paper.

These optimally controlled solutions depend on the δ parameter (the penalizing parameter adjusting the size of the terms in the cost functional), as does the reduction in enstrophy. The controlled state for $\delta=5\times10^{-4}$ corresponding to a corotating roll state [see Figs. 1(a) and 1(b)] can be seen in Figs. 4(a) (isotherms) and 4(b) (velocity field). The corotating rolls have disappeared (the pattern is reduced) and the new controlled state consists of two rolls, one over the other, with a low velocity [$O(10^{-2})$] [see Fig. 4(b)]. Now the enstrophy takes the value 0.06, while for the uncontrolled corotating rolls the value is E=10.69. Thus, there is a considerable reduction of enstrophy in the controlled states. Figure 5 shows the control functions h for different values of δ for the linear flow case. The control function h has an increasing linear profile from the hotter to the colder lateral wall, causing heating of the colder part in the fluid. As δ increases, the control function tends to be zero, i.e., the control function tends to have no effect and the controlled state tends towards an uncontrolled state, as it should be. But for small δ, the control is significant and more effective. Figure 6 shows that for large values of the penalizing parameter δ the enstrophy of the controlled states tends to the enstrophy of the uncontrolled states, while for small values of δ the controlled states have a very small enstrophy. We have seen until now how thermal control through boundaries used to reduce the enstrophy in the flow led to controlled basic states with a clear reduction of patterns [compare Figs. 1(b) and 4(b)].

Regarding to the linear stability analysis of the controlled basic states, the critical Rayleigh numbers depending on δ can be seen in Fig. 7. The bifurcations are stationary. The critical Ra_c for the uncontrolled state is plotted as a horizontal dashed line. This calculation identifies two main characteristics. First, when δ increases, the control has no effect, as noted above, and therefore the threshold tends towards 3245, which is the threshold for the uncontrolled case. Second, for small values of δ ($4.5\times10^{-4}<\delta<6\times10^{-4}$) the threshold is larger than 3245, and there are controlled states which are very strong and never become unstable even if Ra is considerably increased ($\delta<4.5\times10^{-4}$). Then, we have found heat fluxes h (those obtained for $\delta<4.5\times10^{-4}$) such that if we consider them in the Biot boundary condition (5), the corresponding controlled basic states reduce pattern and they are stable for all Ra, i.e., the instability is avoided.

This work was partially supported by Research Grants No. MTM2006-14843-C02-01 (MCYT) and No. PAC-05-005-01 (JCCM), which includes ERDF funds.

[1] S. B. G. M. O'Brien, J. Fluid Mech. **254**, 649 (1993).
[2] T. Okutani *et al.*, Key Eng. Mater. **264-268**, 761 (2004).
[3] N. Postacioglu *et al.*, J. Phys. D **24**, 15 (1991).
[4] J. E. Spinelli *et al.*, J. Alloys Compd. **384**, 217 (2004).
[5] H. Bénard, Rev. Gen. Sci. Pures Appl. **11**, 1261 (1900).
[6] E. Bodenschatz *et al.*, Annu. Rev. Fluid Mech. **32**, 709 (2000).
[7] P. Hirschberg and E. Knobloch, J. Nonlinear Sci. **7**, 537 (1997).
[8] M. K. Smith and S. H. Davis, J. Fluid Mech. **132**, 119 (1983).
[9] S. Hoyas *et al.*, J. Phys. A **35**, 4067 (2002).
[10] A. M. Mancho and H. Herrero, Phys. Fluids **12**, 1044 (2000).
[11] K. Ito and S. S. Ravindran, SIAM J. Sci. Comput. (USA) **19**, 1847 (1998).
[12] H. Herrero and A. M. Mancho, Appl. Numer. Math. **33**, 161 (2000).
[13] H. Herrero and A. M. Mancho, Int. J. Numer. Methods Fluids **39**, 391 (2002).